Revista Española de Cirugía Ortopédica y Traumatología 68 (2024) T262–T270

Revista Española de Cirugía Ortopédica y Traumatología

www.elsevier.es/rot

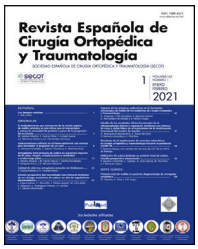

ORIGINAL PAPER

[Translated article] Mechanical resistance of polylactic acid bone matrices developed by 3D printing for the reconstruction of bone defects

A. Ortega-Yago[a,b], J. Ferràs-Tarragó[a,b,*], C. de la Calva-Ceinos[a,b], J. Baeza-Oliete[a,b], M.A. Angulo-Sánchez[a,b], I. Baixauli-García[a,b], F. Arguelles-Linares[a,b], J.V. Amaya-Valero[a,b], F. Baixauli-García[a,b], P. Medina-Bessó[a,b]

[a] *Departamento de Cirugía Ortopédica y Traumatología, Hospital Universitario y Politécnico La Fe, Valencia, Spain*
[b] *Departamento de Fisiología, Universidad de Valencia, Valencia, Spain*

Received 15 December 2022; accepted 1 February 2023
Available online 20 January 2024

KEYWORDS
3D printing;
Bone defects;
Bone matrix;
Bone reconstruction;
3D models

Abstract
Introduction: Bone defects are one of the main limitations in orthopaedic surgery and traumatology. For this reason, multiple bone replacement systems have been developed, either by prosthetic implant or by substitution with osteoforming substances, whose limitations are their survival and lack of structurality, respectively. The objective of this work is the generation of a new material for the creation of biologically active structures that have sufficient tensile strength to maintain the structure during remodelling.
Material and methods: A new filament based on the fusion of natural polylactide acid (PLA) powder was designed for the generation of pieces by means of fused deposition modelling (FDM) on which to carry out tensile mechanical tests of osteosynthesis material. A total of 13 groups with different cortical thickness, filling and layer height were carried out, with 10 tensile tests in each group, defining the tensile breaking limit for each group. The regression lines for each group and their mechanical resistance to traction on the filament used were determined.
Results: The filament ratio per contact surface unit with the osteosynthesis used was the main determinant of the mechanical resistance to traction, either at the expense of the increase in cortical thickness or by the increase in the percentage of cancellous bone filling. Layer height had a minor effect on tensile strength. The regression value was high for cortical thickness and cancellous filling, being elements with a predictable biomechanical behaviour.

DOI of original article: https://doi.org/10.1016/j.recot.2023.02.001
* Corresponding author.
E-mail address: cotferras@gmail.com (J. Ferràs-Tarragó).

https://doi.org/10.1016/j.recot.2024.01.016

Conclusions: The new methodology allows the creation of personalised neutral and implantable PLA bone matrices for the reconstruction of large bone defects by means of 3D printing by FDM with a mechanical resistance to traction greater than that of current biological support structures.

PALABRAS CLAVE
Impresión 3D;
Defectos óseos;
Matrices óseas;
Reconstrucción ósea;
Modelos 3D

Resistencia mecánica de matrices óseas de ácido poliláctico desarrolladas por impresión 3D para la reconstrucción de defectos óseos

Resumen
Introducción: Los defectos óseos son una de las principales limitaciones en cirugía ortopédica y traumatología. Por ello, se han desarrollado múltiples sistemas de sustitución ósea, ya sea mediante implante protésico o mediante sustitución con sustancias osteoformadoras, cuyas limitaciones son su supervivencia y falta de estructuralidad, respectivamente. El objetivo del presente trabajo es la generación de un nuevo material para la creación de estructuras biológicamente activas que dispongan de la resistencia a la tracción suficiente como para mantener la estructura durante la remodelación.
Material y métodos: Se diseñó un nuevo filamento basado en la fusión de ácido poliláctico (PLA) natural en polvo para la generación de piezas mediante el modelado por deposición fundida (FDM) sobre las que se realizaron ensayos mecánicos a tracción de material de osteosíntesis. Se analizaron un total de 13 grupos con distinto grosor cortical, relleno y altura de capa, con 10 ensayos de tracción en cada grupo, definiendo el límite de rotura a la tracción para cada grupo. Se determinaron las rectas de regresión para cada grupo y su resistencia mecánica a la tracción sobre el filamento empleado.
Resultados: El ratio de filamento por unidad de superficie de contacto con la osteosíntesis empleada fue el principal determinante de la resistencia mecánica a la tracción, ya sea a expensas del aumento del grosor cortical o por el aumento en el porcentaje de relleno del hueso esponjoso. La altura de capa tuvo un efecto menor sobre la resistencia a la tracción. El valor de regresión fue alto para el grosor cortical y el relleno de esponjosa, siendo elementos con un comportamiento biomecánico predecible.
Conclusiones: La nueva metodología permite crear matrices óseas personalizadas de PLA neutro implantable para la reconstrucción de grandes defectos óseos mediante impresión 3D por FDM con una resistencia mecánica a la tracción mayor a la de estructuras biológicas de soporte actuales.

Introduction

Bone defects are one of the main limitations for reconstruction in orthopaedic surgery and traumatology.[1] There are multiple reconstruction techniques when a bone defect is present, from allografts to megaprostheses including bone transport techniques, vascularised autografts, pseudomembrane formation, among others.[2–8] The main complications of biological techniques (use of bone substitutes or bone neoformation techniques) are infection (especially in allografts) and lack of consolidation, while the main limitation is survival in non-biological techniques (metallic substitution). The advantage of prosthetic replacement includes the greater speed of the procedure and recovery, while the main advantage of using biological techniques is the greater survival if there are no complications during the process.

There are dozens of osteoinductive materials that allow bone neoformation, from polymers to synthetic ceramics, which enable structural recovery in large bone defects.[3,9] Their main limitation is their mechanical strength, because when used in the patient most of these systems cannot support the load necessary to maintain a functional body part.

Additive manufacturing printing is a manufacturing technique that allows three-dimensional structures to be obtained by fused deposition modelling (FDM) using a thermoplastic material and following a morphology determined by numerical code.[10] Thanks to the patent release of this manufacturing methodology, in the second decade of the 21st century printing machines that use it are experiencing exponential growth. The design software has also been improved, to the point that there are now domestic three-dimensional (3D) structure printers on the market, in common use by the general population. These devices use a filament of variable diameter (depending on the printer), the most common being 1.75 mm, with which objects with practically any morphology can be generated.

Polylactic acid (PLA) is one of the most widely used biocompatible materials for implant design.[6,11,12] PLA is also the most commonly used material for domestic 3D printing, as its fusing temperature is optimal for FDM 3D printers (between 180° and 220° depending on its composition). Its natural form after extraction is a thermosensitive powder and the limitation for the use of PLA filaments already on the market is the presence of substances that can interfere with the osteoinduction process, although some already have the ISO 10993-1 standard for biocompatibility.

There is no filament on the market composed only of natural PLA, because, as it is used to model parts, it is accompanied by different substances that increase its aesthetic appearance and ease of use. However, the additives contraindicate its use for synthesising implantable products. Furthermore, the problem with the use of bioprinters to generate bone matrices is their price and the low mechanical resistance of their products.[6]

The aim of the present work is to generate a filament that can be used by an FDM 3D printing system to obtain mechanically competent structures to provide structural strength to the usual osteoinductive composites currently used in bone defects, and to review other potential applications of these bone matrices in clinical practice, such as in training or planning.

Material and methods

Prospective experimental study developed under in vitro conditions.

Description of the filament generation device

The first key point of the project was the generation of a filament of a constant diameter of around 1.75 mm that would be implementable in a manufacturing FDM 3D printer. For this purpose, we specifically designed a mechanism for synthesising neutral PLA from its natural powder form.

The device consisted of three independent segments:

(a) Powder fusion segment: controlled by temperature sensors and a thermal resistor, it was possible to adjust the fusion temperature. A 1.75 mm nozzle was deployed at the distal end of the fuser to generate a constant diameter.
(b) Powder extrusion segment: the powder was drawn by an endless screw driven by a stepper motor controlled using Arduino® software (Arduino® v.1.8.18 Windows). The endless screw picked up the powder deposited in the nozzle and dragged it to the fuser.
(c) Filament collection system: once the powder was fused, it was collected and wound by means of a spool controlled by numerical code with a stepper motor (Arduino® v.1.8.18 Windows) (Fig. 1).

The speed of the extruder motors and the collection spool were defined to obtain a constant diameter filament of 1.75 mm. To evaluate the filament tolerance, 10 thickness measurements were taken using a gauge, with 20 cm interval between points. The mean filament diameter and the standard deviation between measurements were defined. The target diameter was 1.75 mm with an error tolerance ±.1 mm.

Biomechanical evaluation of the filament

After generating the filament and determining a suitable diameter and tolerance, different cylindrical parts were printed to evaluate the mechanical tensile strength of an osteosynthesis screw inserted into the parts printed in bicortical manner (Fig. 2).

A total of 13 groups of parts were designed in which the layer height, percentage of filling, and wall thickness were modified (Table 1), and the printing time was recorded for each group (Table 1). Ten pieces per group were printed, for a total of 130 mechanical tests. The effect of cancellous bone on tensile strength was evaluated by modifying the model filling, comparing groups 1–5. To evaluate the effect of layer height, tensile strength was compared between groups 6–9 and groups 10–13 were compared to evaluate the effect of cortical thickness (Table 1).

To define the tensile strength, it was subjected to a tensile test in a testing machine (PCE MTS500, PCE Ibérica®) and the breaking limit was evaluated by dynamometer (PCE-DFG N 5K), defining the maximum supported force as the variable of interest with a resolution of 1N and an accuracy of ±.1%.

The contact area of the screw with the filament was evaluated, considering a constant section of 6 mm and a screw length of 30 mm. Thus, the pressure supported per contact surface unit in each of the configurations was determined.

Statistical analysis

A descriptive analysis of the mean and standard deviation was made for each of the groups. The statistical analysis was performed for a β error of .2, an α error of .05, a precision for the detection of variation between groups of 2000 kPa, and a standard deviation of 5% with respect to the mean, in accordance with previous exploratory studies.

''Normal'' or ''Non-normal'' behaviour of the data was analysed using the Lilliefors test, assuming ''Normality'' with p-values greater than .05.

A linear regression test was used to analyse the relationship between the filling value, layer height, and cortical thickness, with the supported strength, because the data behaviour was ''Normal''. Therefore, an equation for biomechanical prediction was performed according to the evaluated parameter.

Statistical analysis was performed using R version 4.2.1 ''Funny-Looking Kid'' software.

Results

The progressive increase in the filling of the biomodel produced a linear increase in tensile strength, which was the linear behaviour and the model predictor (R^2 = .89; *p*-value <.01; Table 2A and Fig. 3A). The standard deviation of the groups was significantly greater with the increase in tensile strength required to produce mechanical failure (*p*-value <.01).

Table 1 Description of the parameters of the groups used for biomechanical analysis A, B.

Group	Layer height	Cortical thickness	Number of upper layers	Number of lower layers	Density of filling	Lateral wall thickness	Number of wall lines	Printing time (min)	Filling pattern	Metres of filament	Grams of filament
1	.3	1	4	4	0	2	5	423	Gyroid	27.26	81
2	.3	1	4	4	15	2	5	544	Gyroid	36.7	109
3	.3	1	4	4	30	2	5	727	Gyroid	45.99	137
4	.3	1	4	4	45	2	5	898	Gyroid	55.4	165
5	.3	1	4	4	60	2	5	1202	Gyroid	63.64	190
6	.1	1	4	4	15	2	5	1556	Gyroid	36.42	109
7	.2	1	4	4	15	2	5	788	Gyroid	36.24	108
8	.4	1	4	4	15	2	5	411	Gyroid	36.38	109
9	.5	1	4	4	15	2	5	325	Gyroid	35.33	105
10	.3	2	7	7	15	2	5	599	Gyroid	40.1	120
11	.3	3	10	10	15	2	5	652	Gyroid	43.49	130
12	.3	4	14	14	15	2	5	722	Gyroid	47.99	143
13	.3	5	17	17	15	2	5	776	Gyroid	51.39	153

Group	Bicortical cortical contact area	Monocortical cortical contact area	Cancellous contact area	Total bicortical contact area	Total monocortical contact area
1	18.84	9.42	0	18.84	9.42
2	18.84	9.42	79.128	97.968	88.548
3	18.84	9.42	158.256	177.096	167.676
4	18.84	9.42	237.384	256.224	246.804
5	18.84	9.42	316.512	335.352	325.932
6	18.84	9.42	79.128	97.968	88.548
7	18.84	9.42	79.128	97.968	88.548
8	18.84	9.42	79.128	97.968	88.548
9	18.84	9.42	79.128	97.968	88.548
10	37.68	18.84	73.476	111.156	92.316
11	56.52	28.26	67.824	124.344	96.084
12	75.36	37.68	62.172	137.532	99.852
13	94.2	47.1	56.52	150.72	103.62

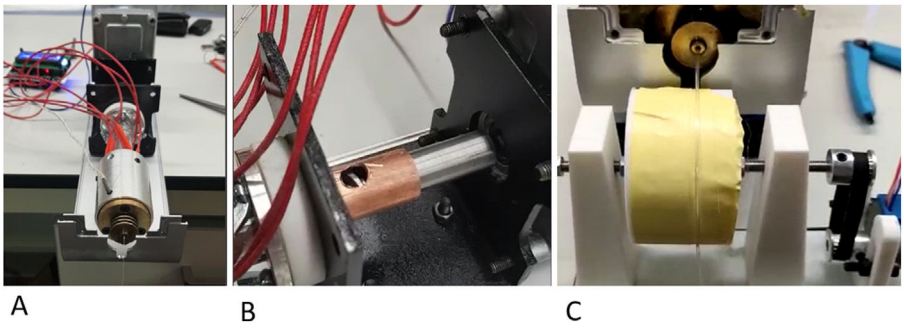

Figure 1 Device for filament synthesis with pure polylactic acid. (A) Longitudinal view of the device. (B) Nozzle through which the PLA powder is introduced. (C) Filament collection and winding system.

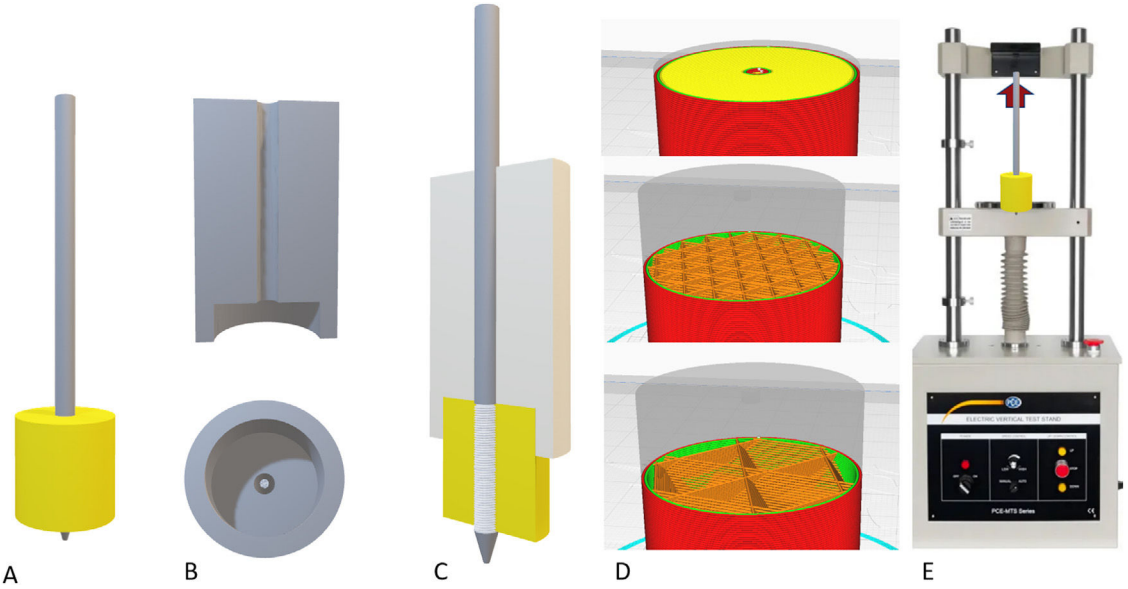

Figure 2 Assembly of the models for the loading tests. (A) Final assembly with the coil (30 mm) completely inserted into the model. (B) System used to insert the pin perfectly perpendicular to the model. (C) Definitive assembly of the pin on the model, keeping the insertion piece. (D) Examples of the cortical pattern (top), cancellous with 30% filling (centre) and with 10% filling (bottom). (E) Sample of the tensile test scenario.

Table 2 Description of the parameters of the groups used for the biomechanical analysis.

Filling	Mean	SD	IQR	Median	Contact area
0	1962	195.24	300	2030	18.840
15	7434.28	1069.84	1190	7570	97.968
30	10926.57	1489.80	1765.5	10432	177.096
45	15080	2315.65	3020	15650	25.224
60	16950	2455.02	2175	16735	335.352

Filling	Mean	SD	IQR	Median
0	104.14013	10.363240	15.923567	107.74947
15	75.88484	10.920321	12.146823	77.27013
30	61.69858	8.412419	9.969169	58.90590
45	58.85475	9.037627	11.786562	61.07937
60	50.54391	7.320732	6.485722	49.90279

IQR: interquartile range; SD: standard deviation.
A: mean maximum strength (kPa) of the different groups. B: mean maximum pressure (strength per contact surface unit) supported by each of the groups.

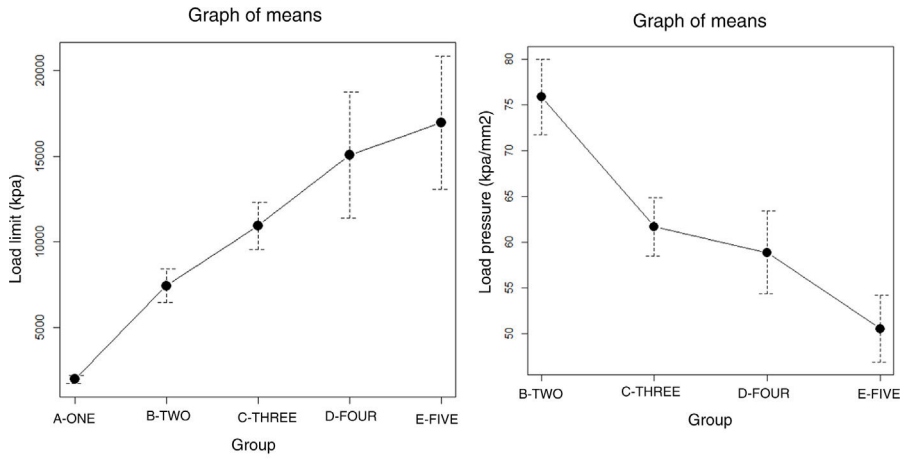

Figure 3 (A) Plot of tensile strength means in each of the groups with variable filling. (B) Ratio of strength per contact area in groups 2–5.

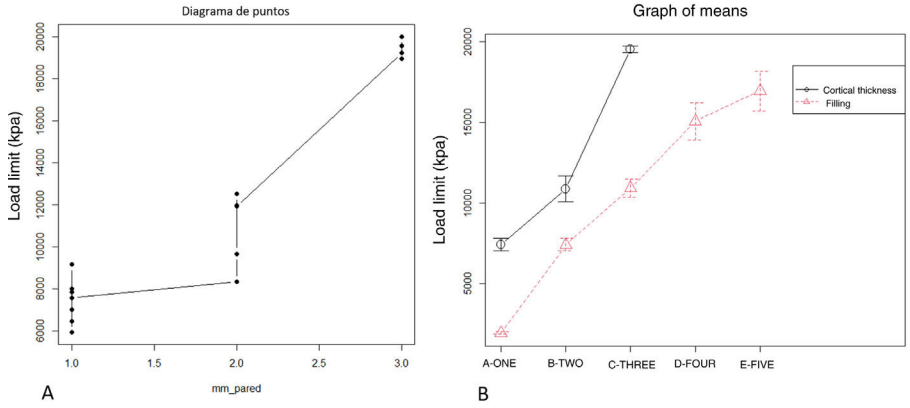

Figure 4 (A) Plot of the mean tensile strength in each of the groups with different cortical thickness. (B) Ratio of strength per surface area between groups with variable filling and variable cortical thickness. Cortical thickness had a greater influence on tensile strength.

The ratio of strength supported per contact surface unit remained similar between the groups with variable filling (p-value = .34; Table 2B and Fig. 4B), with the exception of group 1, in which the strength per contact surface unit was significantly higher than the rest of the groups (p-value .034).

The increase in cortical area involved the greatest increase in tensile strength between groups (p-value <.01) so that the increase of less than 10% produced an increase in tensile strength that was practically double (Table 1 and Fig. 4). The behaviour between mm of cortical thickness and tensile strength presented a linear behaviour with a high level of correlation (R^2 = .89; p-value <.01), producing the maximum level of strength defined prior to the study in the third test group with a cortical thickness of 3 mm (Fig. 4).

The increase in layer height reduced the mechanical tensile strength with a linear ratio and a low degree of predictability (R^2 = .57; p-value <.001). The grams of filament used for each group did not show significant differences, while the time taken for each group was statistically higher (p-value <.01).

The increase in tensile strength was directly related to the area of contact between the screw and the filament, regardless of whether the contact was in the cancellous (filled) or cortical area (R^2 = .76; p-value <.01, Fig. 5).

Discussion

The mechanical strength of matrices printed by PLA FDM is directly related to the printing parameters used, the main factor determining its strength being the ratio of filament per contact surface unit with the osteosynthesis used. We can increase the ratio by increasing the filament content in the central zone or in the cortical zone, which are equivalent in terms of their effect on tensile strength.

The maximum strength achieved by the proposed fabrication system is about 20,000 kPa, which is similar in strength to that of healthy bone tissue, this tensile strength is therefore sufficient for clinical use.[13] Thus, the matrix generated using the filament could provide structurality to the rest of the elements that would be combined inside the mesh. Since almost any morphology can be generated by FDM

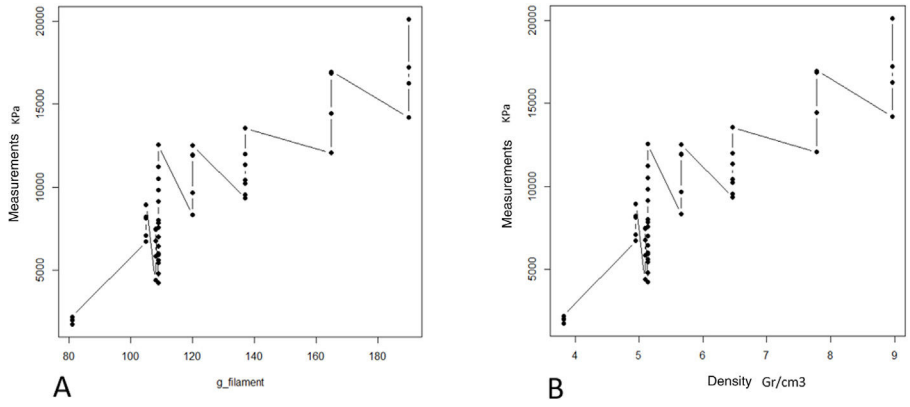

Figure 5 (A) Dot plot between the increase in filament used for model construction and tensile strength, regardless of filament arrangement. (B) Dot plot between density (g/cm^3) of the model and tensile strength, regardless of its arrangement.

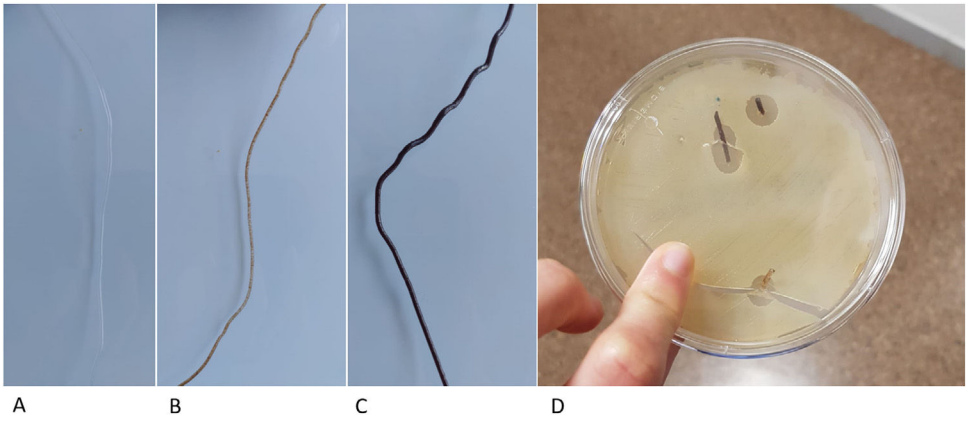

Figure 6 PLA filament loaded with different substances. (A) Neutral PLA filament. (B) Filament with 10% hydroxyapatite content, ready to be used for the creation of matrices with FDM printers. (C) Filament with 30% hydroxyapatite. (D) Vancomycin-loaded filament in a Petri dish with vancomycin-sensitive pathogens.

manufacturing, meshes could be designed to support any osteoinductor on the market, with the mesh providing the structure and the osteoinductive substance the function.

Previous studies have developed other systems for the synthesis of PLA-based matrices constructed using FDM technology,[14] which generate the structure directly from the powder, which is extruded through specific bioprinter fusers[15] and contains substances that can interfere with the osteoinduction process. In contrast, our protocol proposes the generation of a neutral and therefore implantable PLA filament, of constant diameter, by means of a device specifically designed for this purpose. This filament has better biomechanical resistance results and can also be used in conventional 3D printers, significantly reducing the manufacturing price and, therefore, improving its accessibility in clinical practice. Another added advantage of using neutral PLA is the ability to incorporate biologically active substances into a matrix that provides structurality, such as osteoinductive substances, antibiotics, and antineoplastics. By controlling porosity and internal structure, it is possible to customise the content of the matrix, providing an opportunity for new lines of research (Fig. 6).

There are previous studies on the use of PLA as a base for the incorporation of biologically active substances such as hyaluronic acid[14] or bioviodria,[15] with promising results regarding the maintenance of the activity of the incorporated substances. The main advantage of using FDM technology from a natural PLA filament is the simplicity of the printing process, which has a direct impact on its cost, as the methodology is accessible at hospital level. Therefore, this technology is promising for the reconstruction of large bone defects and for treatment with local pharmacological therapies.

The use of 3D biomodels for preoperative planning is also useful in predicting sufficient stability of an osteosynthesis construct. The use of finite element simulations is complex, as it requires long series of similar patients to establish a mathematical model, which is complex in traumatology due to the large number of different fracture patterns and patients encountered.[16] This is why most studies continue to recommend the use of simulations on real models.[17] By using defined printing protocols, it is possible to generate biomodels that are mechanically similar to the resistance of a specific patient, and mechanical tests can be performed

to determine the optimal osteosynthesis configuration prior to surgery.[13] Thanks to new imaging techniques, we can reliably estimate the mechanical strength of a patient's bone, adapting the configuration of the printed biomodel to the data obtained by imaging techniques.[18,19]

The main limitations of the present work are, on the one hand, the lack of biomechanical evaluation in long loading cycles, and on the other, the lack of compression and rotation tests. Our aim is to generate matrices that behave similarly to healthy bone and, given the lack of biomechanical studies with repetition cycles in healthy bone, we opted to evaluate a single tensile test in order to make a qualitative comparison with the present data, although the in vivo behaviour is much more complex.[20] Resistance to axial compression and rotation is decisive for any implant. However, the matrices we propose are fixed to the defect area by means of osteosynthesis material, which would support most of the mechanical resistance until consolidation. Therefore, we did not perform mechanical tests in the three axes of space, although this would be interesting for future studies.

This is the first mechanical validation study on the filament that we present, its clinical utility is still some time away. In future studies, we will evaluate the influence that the PLA degradation of our matrix may have on the osteoinductive components included in it, and on implantable drugs.

In conclusion, we describe in this study a new methodology for the creation of customisable meshes for the reconstruction of large bone defects using FDM 3D printing technology, employing implantable neutral PLA, with a higher mechanical tensile strength than current support structures.

Level of evidence

Level of evidence III.

Funding

The work received funding from the Spanish Society of Orthopaedic and Trauma Surgery through the grants for introduction to research (2020) and from the AO Foundation through its research grants (2021). The project was financed through national funds for research from the centre for industrial development (CDTI) in collaboration with the innovation and development department of Surgival SA.

Conflict of interests

The authors have no conflict of interests to declare.

References

1. Nauth A, Schemitsch E, Norris B, Nollin Z, Watson J. Critical-size bone defects: is there a consensus for diagnosis and treatment? J Orthop Trauma. 2018;32 Suppl. 3:S7–11, http://dx.doi.org/10.1097/BOT.0000000000001115.
2. Baldwin P, Li D, Auston D, Mir H, Yoon R, Koval K. Autograft, allograft, and bone graft substitutes: clinical evidence and indications for use in the setting of orthopaedic trauma surgery. J Orthop Trauma. 2019;33:203–13, http://dx.doi.org/10.1097/BOT.0000000000001420.
3. El-Rashidy AA, Roether JA, Harhaus L, Kneser U, Boccaccini AR. Regenerating bone with bioactive glass scaffolds: a review of in vivo studies in bone defect models. Acta Biomater. 2017;62:1–28, http://dx.doi.org/10.1016/j.actbio.2017.08.030.
4. Ma H, Feng C, Chang J, Wu C. 3D-printed bioceramic scaffolds: from bone tissue engineering to tumor therapy. Acta Biomater. 2018;79:37–59, http://dx.doi.org/10.1016/j.actbio.2018.08.026.
5. Rahmani M, Khani M, Rabbani S, Mashaghi A, Noorizadeh F, Faridi-Majidi R, et al. Development of poly (mannitol sebacate)/poly (lactic acid) nanofibrous scaffolds with potential applications in tissue engineering. Mater Sci Eng C Mater Biol Appl. 2020;110:110626, http://dx.doi.org/10.1016/j.msec.2020.110626.
6. Tack P, Victor J, Gemmel P, Annemans L. 3D-printing techniques in a medical setting: a systematic literature review. Biomed Eng Online. 2016;15:115, http://dx.doi.org/10.1186/s12938-016-0236-4.
7. Wen Y, Xun S, Haoye M, Baichuan S, Peng C, Xuejian L, et al. 3D printed porous ceramic scaffolds for bone tissue engineering: a review. Biomater Sci. 2017;5:169–98.
8. Zhang L, Yang G, Johnson BN, Jia X. Three-dimensional (3D) printed scaffold and material selection for bone repair. Acta Biomater. 2019;84:16–33, http://dx.doi.org/10.1016/j.actbio.2018.11.039.
9. Han SH, Cha M, Jin Y, Lee K, Lee JH. BMP-2 and hMSC dual delivery onto 3D printed PLA-biogel scaffold for critical-size bone defect regeneration in rabbit tibia. Biomed Mater. 2020;16:015019, http://dx.doi.org/10.1088/1748-605X/aba879.
10. Zhu W, Ma X, Gou M, Mei D, Zhang K, Chen S. 3D printing of functional biomaterials for tissue engineering. Curr Opin Biotechnol. 2016;40:103–12, http://dx.doi.org/10.1016/j.copbio.2016.03.014.
11. Santoro M, Shah SR, Walker JL, Mikos AG. Poly(lactic acid) nanofibrous scaffolds for tissue engineering. Adv Drug Deliv Rev. 2016;107:206–12, http://dx.doi.org/10.1016/j.addr.2016.04.019.
12. Singh NK, Han W, Nam SA, Kim JW, Kim JY, Kim YK, et al. Three-dimensional cell-printing of advanced renal tubular tissue analogue. Biomaterials. 2020;232:119734, http://dx.doi.org/10.1016/j.biomaterials.2019.119734.
13. Oftadeh R, Perez-Viloria M, Villa-Camacho JC, Vaziri A, Nazarian A. Biomechanics and mechanobiology of trabecular bone: a review. J Biomech Eng. 2015;137, http://dx.doi.org/10.1115/1.4029176.
14. Farsi M, Asefnejad A, Baharifar H. A hyaluronic acid/PVA electrospun coating on 3D printed PLA scaffold for orthopedic application. Prog Biomater. 2022;11:67–77, http://dx.doi.org/10.1007/s40204-022-00180-z.
15. Brézulier D, Chaigneau L, Jeanne S, Lebullenger R. The challenge of 3D bioprinting of composite natural polymers PLA/bioglass: trends and benefits in cleft palate surgery. Biomedicines. 2021;9:1553, http://dx.doi.org/10.3390/biomedicines9111553.
16. Guha I, Zhang X, Rajapakse CS, Chang G, Saha PK. Finite element analysis of trabecular bone microstructure using CT imaging and continuum mechanical modeling. Med Phys. 2022;49:3886–99, http://dx.doi.org/10.1002/mp.15629.

17. Thomrungpiyathan T, Luenam S, Lohwongwatana B, Sirichativapee W, Nabudda K, Puncreobutr C. A custom-made distal humerus plate fabricated by selective laser melting. Comput Methods Biomech Biomed Engin. 2021;24:585–96, http://dx.doi.org/10.1080/10255842.2020.1840560.
18. Campbell GM, Glüer C. Skeletal assessment with finite element analysis: relevance, pitfalls and interpretation. Curr Opin Rheumatol. 2017;29:402–9, http://dx.doi.org/10.1097/BOR.0000000000000405.
19. MacNeil JA, Boyd SK. Bone strength at the distal radius can be estimated from high-resolution peripheral quantitative computed tomography and the finite element method. Bone. 2008;42:1203–13, http://dx.doi.org/10.1016/j.bone.2008.01.017.
20. Kelly NH, Schimenti JC, Ross FP, van der Meulen MCH. Transcriptional profiling of cortical versus cancellous bone from mechanically-loaded murine tibiae reveals differential gene expression. Bone. 2015;86M:22–9, http://dx.doi.org/10.1016/j.bone.2016.02.007.